Unusual smectic phases organized by novel λ-shaped mesogenic molecules†

Akihisa Yamaguchi,[a] Isa Nishiyama,[b] Jun Yamamoto,[b] Hiroshi Yokoyama[b] and Atsushi Yoshizawa*[a]

Received 4th May 2004, Accepted 9th September 2004
First published as an Advance Article on the web 23rd September 2004
DOI: 10.1039/b406716a

A homologous series of novel λ-shaped mesogenic compounds in which three mesogenic groups are connected to 3, 4-dihydroxybenzoic acid has been prepared and their physical properties investigated by means of optical microscopy, differential scanning calorimetry and X-ray diffraction measurements. The λ-shaped compounds studied showed unusual smectic phases. 4-Cyanobiphenyl-4′-yl 3,4-bis{6-[4-(5-octylpyrimidin-2-yl)phenyloxy]hexyloxy}benzoate was found to realize an incommensurate SmA (SmAinc) phase. A "uniform planarly" aligned sample of 2-(4-octylphenyl)pyrimidin-5-yl 3,4-bis{6-[4-(5-octylpyrimidin-2-yl)phenyloxy]hexyloxy} benzoate showed a Schlieren-like texture in the smectic phase. We discuss structural effects of the λ-shaped compounds on molecular organization in liquid-crystalline phases.

The driving force of mesophase formation is a fundamental topic in the investigation of molecular assembly systems. Recently, molecular topology[1] and microsegregation[2] have attracted much attention as the origins for producing novel self-organizing systems. For example, "Janus-like" supermolecular liquid crystals, with molecular weights in excess of 4000 D, have been introduced as a new style of molecular topology, and have been found to exhibit chiral nematic and chiral smectic C (SmC*) phases.[3] Novel layered structures have also been realized by the microsegregation effect produced by newly designed mesogenic block molecules carrying a semiperfluorinated chain.[4] In addition to these static features of the molecular structures, molecular motion is also important to understand the microscopic behaviour of mesogenic molecules. Our ^{13}C NMR studies of smectic liquid crystals give a new concept for molecular design of liquid crystals.[5] Coupling or competition between intra-layer core–core interaction and inter-layer interaction can produce a new class of molecular aggregation. We have reported an unusual endothermic SmC* to cubic phase transition in a dichiral compound,[6] layered structure in the nematic (N) phase consisting of U-shaped molecules[7] and a novel frustrated phase produced by a binary system of non-symmetric liquid crystals.[8] In these previous studies, it was found that (1) the endothermic transition is organized by chiral recognition as a result of frustration between inter-layer and intra-layer interactions, (2) the layered ordering in the N phase is attributed to strong correlation of core parts between the mesogenic groups of each U-shaped molecule, and (3) the novel frustrated phase observed in the binary system results from frustration between core–core interactions and molecular packing. We report here the design and properties of novel λ-shaped mesogenic molecules. Fig. 1 shows the design concept of the λ-shaped system. The λ-shaped molecular topology (Fig. 1 (b)) is expected to produce a characteristic effect since two different non-symmetric dimeric molecular configurations (*i.e.*, one is a straight-shaped configuration (Fig. 1 (a)) and the other a bent structure (Fig. 1 (c))) co-exist in a single mesogenic molecule.

Experimental

Spectroscopic analysis

Purification of final products was carried out using column chromatography over silica gel (63–210 μm) (Kanto Chemical Co., Inc.) using dichloromethane or a dichloromethane–ethyl acetate mixture as the eluent, followed by the recrystallization from ethanol. The purities of all of the final compounds were checked by normal phase HPLC (Intersil SIL 150A-5 column). A dichloromethane–isopropylalcohol (85 : 15) mixture was used as eluent. Detection of products was achieved by UV irradiation (λ = 254 nm). The structures of the final products were elucidated by infrared (IR) spectroscopy (BIO RAD FTS-30) and proton nuclear magnetic resonance (^{1}H NMR) spectroscopy (JEOL JNM-GX270).

Preparation of materials

Ethyl 3,4-bis{6-[4-(5-octylpyrimidin-2-yl)phenyoxy]hexyloxy}benzoate. 5-Octyl-2-(4-hydroxyphenyl)pyrimidine (0.57 g, 2.0 mmol) purchased from Midori Kagaku Co., Ltd. and 1, 6-dibromohexane (0.73 g, 3.0 mmol) were dissolved in cyclohexanone (10 mL). Potassium carbonate (0.28 g, 2.0 mmol) was then added and the resulting mixture was stirred at 80 °C for 6 h. The reaction mixture was filtered and the solvent was removed by evaporation under reduced pressure. The product was purified by column chromatography using

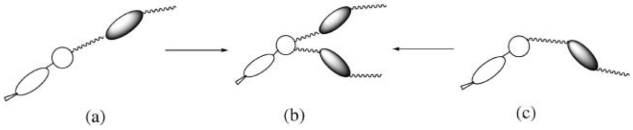

Fig. 1 Design concept of the λ-shaped mesogenic molecule.

---

† Electronic supplementary information (ESI) available: Details of material preparation. See http://www.rsc.org/suppdata/jm/b4/b406716a/

*ayoshiza@cc.hirosaki-u.ac.jp

dichloromethane as the eluent. 2-[4-(6-Bromohexyloxy)-phenyl]-5-octylpyrimidine was obtained. Yield: 0.56 g (63%).

2-[4-(6-Bromohexyloxy)phenyl]-5-octylpyrimidine (1.1 g, 2.5 mmol) and ethyl 3,4-dihydroxybenzoate (0.23 g, 1.25 mmol) were dissolved in cyclohexanone (15 mL). K_2CO_3 (0.69 g, 5.0 mmol) and KI (0.0.42 g, 0.25 mmol) were then added and the resulting mixture was stirred at 145 °C for 14 h. The reaction mixture was filtered and the solvent was removed by evaporation under reduced pressure. The product was purified by column chromatography using a dichloromethane–ethyl acetate (20 : 1) mixture as the eluent, and recrystallized from an ethanol–chloroform (4 : 1) mixture (10 mL). Yield: 0.83 g (73%).

δ_H (270 MHz, $CDCl_3$, TMS): 8.55 (s, 4 H, Ar–H), 8.34 (d, 4 H, Ar–H, J = 9.2 Hz), 7.64 (dd, 1 H, Ar–H, J = 8.6 Hz, 1.9 Hz), 7.55 (d, 1 H, Ar–H, J = 1.9 Hz), 6.96 (d, 4 H, Ar–H, J = 8.6 Hz), 6.87 (d, 1 H, Ar–H, J = 8.4 Hz), 4.34 (q, 2 H, $-COOCH_2-$, J = 7.3 Hz), 4.06 (t, 4 H, $-OCH_2-$, J = 6.5 Hz), 4.02 (t, 4 H, $-OCH_2-$, J = 6.5 Hz), 2.58 (t, 4 H, Ar–CH_2–, J = 7.6 Hz), 1.87–1,27 (m, 43 H, aliphatic-H), 0.88 (t, 6 H, $-CH_3$, J = 6.8 Hz). ν/cm^{-1}(KBr): 2925, 2852 (C–H str.), 1717 (–CO–O–C– str.), 1611, 1597 (C=C str.).

3,4-Bis{6-[4-(5-octylpyrimidin-2-yl)phenyloxy]hexyloxy}benzoic acid. Ethyl 3,4-bis{6-[4-(5-octylpyrimidin-2-yl)phenyloxy]-hexyloxy}benzoate (0.83 g, 0.91 mmol) was added to a solution of KOH (0.50 g, 8.9 mmol) in ethanol (95%, 20 mL). The resulting mixture was stirred under reflux for 2 h. The solution was acidified with aq. HCl. Water (20 mL) was added to the mixture and the aqueous phase was extracted with dichloromethane (3 × 20 mL). The organic extracts were combined, dried over Na_2SO_4, filtered and evaporated. Yield: 0.72 g (89%).

δ_H (270MHz, $CDCl_3$, TMS): 8.57 (s, 4 H, Ar–H), 8.33 (dd, 4 H, Ar–H, J = 8.4 Hz, 2.6 Hz), 7.72 (dd, 1 H, Ar–H, J = 8.4 Hz, 2.0 Hz), 7.59 (d, 1 H, Ar–H, J = 2.2Hz), 6.96 (dd, 4 H, Ar–H, J = 8.9 Hz,1.4 Hz), 6.89 (d, 1 H, Ar–H, J = 8.4 Hz), 4.10–4.00 (m, 8 H, $-OCH_2-$), 2.58 (t, 4 H, Ar–CH_2–, J = 7.7 Hz), 1.87–1.27 (m, 40 H, aliphatic-H), 0.88 (t, 6H, $-CH_3$, J = 6.8 Hz). ν/cm^{-1}(KBr): 2927, 2854 (C–H str.), 1680 (C=O str. –COOH),1607, 1585 (C=C str.).

4-Cyanobiphenyl-4′-yl 3,4-bis{6-[4-(5-octylpyrimidin-2-yl)phenyloxy]hexyloxy}benzoate, 4. To a solution of 3,4-bis{6-[4-(5-octylpyrimidin-2-yl)phenyloxy]hexyloxy}benzoic acid (0.20 g, 0.23 mmol) in dichloromethane (15 mL), 4-cyano-4′-hydroxybiphenyl (0.044 g, 0.23 mmol), dicyclohexylcarbodiimide (0.047 g, 0.23 mmol), and 4-(*N*,*N*-dimethylamino)pyridine (0.003g, 0.023 mmol) were added. The resulting solution was stirred at room temperature overnight. Precipitated materials were removed by filtration. After removal of the solvent by evaporation, the residue was purified by column chromatography on silica gel (using a dichloromethane–ethyl acetate (20 : 1) mixture as the eluent). Recrystallization from an ethanol–chloroform (5 : 1) mixture (6 mL) gave the desired product. Yield: 0.16 g (68%).

δ_H (270MHz, $CDCl_3$, TMS): 8.56 (d, 4 H, Ar–H, J = 1.4 Hz), 8.34 (dd, 4 H, Ar–H, J = 8.9 Hz, 3.0 Hz), 7.83 (dd, 1 H, Ar–H, J = 8.5 Hz, 2.2 Hz), 7.74–7.60 (m, 7 H, Ar–H), 7.33 (d, 2 H, Ar–H, J = 8.9 Hz), 6.99–6.94 (m, 5 H, Ar–H), 4.11 (t, 2 H, $-OCH_2-$, J = 6.5 Hz), 4.10 (t, 2 H, $-OCH_2-$, J = 6.5 Hz), 4.03 (t, 2 H, $-OCH_2-$, J = 6.5 Hz), 4.02 (t, 2 H, $-OCH_2-$, J = 6.5 Hz), 2.58 (t, 4 H, Ar–CH_2–, J = 7.7 Hz), 1.90–1.27 (m, 40 H, aliphatic-H), 0.88 (t, 6 H, $-CH_3$, J = 6.6 Hz). ν/cm^{-1}(KBr): 2925, 2852 (C–H str.), 1608, 1583 (C=C str.). Purity: 100%.

Details of material preparation for the other compounds are listed in the electronic supplementary information (ESI)†.

Liquid-crystalline and physical properties

The initial phase assignments and corresponding transition temperatures for the final products were determined by optical polarized light microscopy using a Nikon Optiphoto POL polarizing microscope equipped with a Mettler FP82 hot stage and FP80 control processor. The heating and cooling rates were 5 °C min^{-1}. The photomicrographs were taken using a camera (Olympus Digital Camera C-5050 ZOOM) in conjunction with a Nikon Optiphoto POL polarizing microscope. Temperatures and enthalpies of transition were investigated by differential scanning calorimetry (DSC) using a Seiko Instruments Inc. DSC6200. The materials were studied at a scanning rate of 2–10 °C min^{-1} after being encapsulated in aluminum pans.

The X-ray scattering experiments were performed using a real-time X-ray diffractometer (Bruker AXS D8 Discover). The monochromatic X-ray beam (Cu Kα line) was generated by a 1.6 kW X-ray tube and Göbel mirror optics. The 2D position sensitive detector has 1024 × 1024 pixels in a 5 cm × 5 cm beryllium window. A sample was introduced into a thin glass capillary tube (diameter 1.0 mm), which was placed in a custom-made temperature stabilized holder (stability within ±0.1 °C). The X-ray diffraction measurements and the textural observations by polarized light microscopy using a CCD camera were performed simultaneously on the sample in the glass capillary tube.

Results and discussion

Liquid-crystalline properties

Molecular structures and transition properties of the λ-shaped mesogenic compounds are shown in Fig. 2. Compound **1** showed the phase sequence of Iso–N–SmA–SmC, on the other hand, compound **2** with a biphenyl as X showed only a N phase, suggesting that lack of inter-layer permeation of tails for compound **2** destabilizes the layer ordering. Compound **3** having a chiral centre showed only a SmA phase. Texture at the Iso–SmA transition for compound **3** seems to be different from a typical fan-shaped texture of a SmA phase (Fig. 3). On cooling from the istropic liquid, coloured curved stripes appeared. Then they grew and curled up. A similar texture has been reported in the chiral non-symmetric dimeric liquid crystal (10B5T8*),[9] and also in the achiral liquid crystal compound.[10] The racemic mixture between (*R*)- and (*S*)-isomers of compound **3** also showed the unusual texture at the Iso–SmA transition. Thus, the unusual texture of compound **3** (see Fig. 3) is thought not to be produced by the chirality-dependent effect but is attributable to the layer

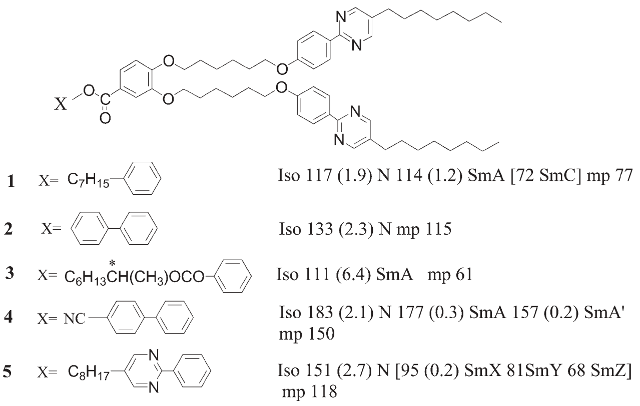

1 Iso 117 (1.9) N 114 (1.2) SmA [72 SmC] mp 77

2 Iso 133 (2.3) N mp 115

3 Iso 111 (6.4) SmA mp 61

4 Iso 183 (2.1) N 177 (0.3) SmA 157 (0.2) SmA' mp 150

5 Iso 151 (2.7) N [95 (0.2) SmX 81SmY 68 SmZ] mp 118

Fig. 2 Molecular structures, transition temperatures/°C and $\Delta S/R$ (in parenthesis) of the λ-shaped mesogenic compounds. Square brackets indicate a monotropic transition.

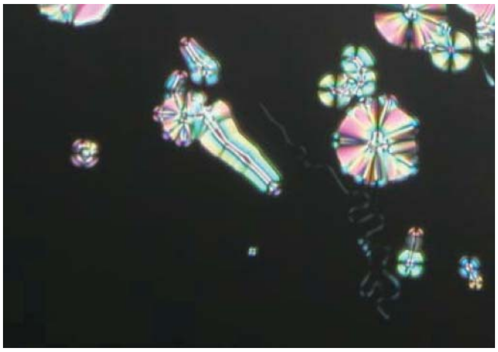

Fig. 3 A photomicrograph of a texture of compound **2** on cooling from the isotropic liquid phase. Magnification 100 ×.

deformation induced by the λ-shaped structure of compound **3** at the direct transition from isotropic liquid to SmA phase.

Compound **4** showed two smectic A phases, designated as SmA and SmA′. Both of the SmA and SmA′ phases showed a homeotropic texture as usually observed for common smectic A phases, which was completely dark under the polarized light microscopy. However, the planar unidirectionally aligned SmA′ phase exhibited an anomalous texture with many defects (Fig. 4). The SmA–SmA′ phase transition was also confirmed by means of differential scanning calorimetry (Fig. 5). A small but clear peak was obtained at the transition, indicating that the SmA and SmA′ phases are two thermodynamically different phases.

Compound **5** in which a phenylpyrimidine moiety is introduced as X showed three unusual smectic phases, *i.e.*, SmX, SmY and SmZ phases. Microscopic observation on a homeotropically aligned sample revealed that the N and SmX phases are optically uniaxial phases. However, the SmY and SmZ phases did not show the homeotropic texture but showed some patterns due to the increase of the birefringence, indicating that they are biaxial phases (Fig. 6 (a) and (b)), where clearly different textures were observed between the SmY and SmZ phases. A Schlieren texture was observed in the uniform planarly aligned N phase as usual (Fig. 7 (a)). Furthermore, a Schlieren-like texture was also observed in the

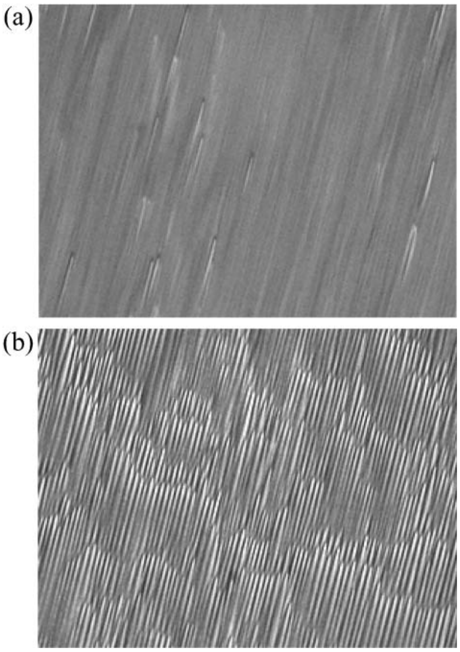

Fig. 4 Photomicrographs of (a) the SmA phase at 170 °C and (b) the SmA′ phase at 150 °C of a planar unidirectionally aligned sample of compound **4**.

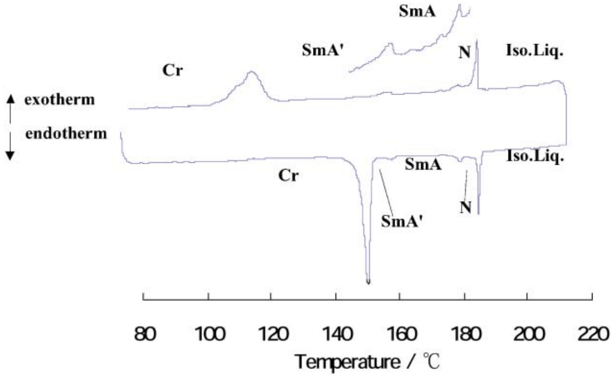

Fig. 5 DSC thermogram for compound **4**. The rate of cooling and heating was 5 °C min^{-1}.

SmX, SmY and SmZ phases of a uniform planarly aligned region on cooling from the N phase (Fig. 7 (b), (c) and (d), respectively). A Schlieren texture in smectic phases, which results from deformation of the c-director, is usually observed in a pseudo-homeotropically aligned sample of tilted smectic phases; however, the Schlieren-like texture this time was observed in the smectic phases of the uniform planarly aligned sample. The phase transition behaviour of compound **5** was also examined by DSC measurement. Fig. 8 shows a cooling DSC thermogram for compound **5**, where a small peak at the N to SmX transition was observed, on the other hand, enthalpy changes associated with the SmX to SmY and SmY to SmZ transitions could not be detected.

Let us discuss the nematic–isotropic transition entropies. The transition entropy is made up of two contributions, one resulting from the onset of long range orientational order and

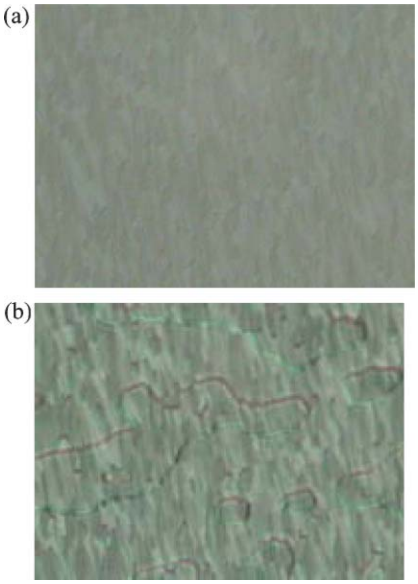

Fig. 6 Photomicrographs of (a) the SmY phase at 75 °C and (b) the SmZ phase at 60 °C of a homeotropically aligned sample of compound **5**. Magnification 100 ×.

the other from the change in the conformational composition.[11] For rigid and rod-like molecules, $\Delta S/R$ should be about 0.3. On the other hand, the N–I transition for dimeric compounds is considerably larger than for the monomeric compounds. Furthermore, the transition entropies show a pronounced alternation as parity of the spacer is varied. The values for the N–I transition entropy for even members are typically several times larger than those for the odd members. The observed transition entropies for the λ-shaped molecules, for example, 1.94 for compound **1** and 2.72 for compound **5**, are much larger than those for rod-like molecules. These large values suggest that the λ-shaped molecules are behaving as dimeric molecules, which is thought to reflect the design concept as shown in Fig. 1.

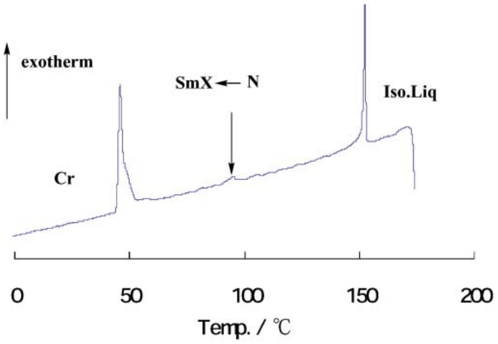

Fig. 8 Cooling DSC thermogram for compound **5**. The rate of cooling was 5 °C min^{-1}.

Phase structures

Compounds 1 and 3

Layer spacings in the SmA phase of about 40 Å and 41 Å were obtained for compounds **1** and **3**, respectively, from X-ray diffraction (XRD) measurements. Molecular lengths were estimated, from MM2 models, to be about 46 Å and 49 Å for compounds **1** and **3**, respectively. Thus, compounds **1** and **3** are considered to form a monolayer SmA phase in which interlayer permeation of the tails is thought to occur. The smectic layer spacing calculated form the X-ray reflection of compound **1** changed from 40 Å at 73.2 °C in the SmA phase to 39 Å at 68.5 °C in the SmC phase.

Compound 4

Fig. 9 shows X-ray diffraction profiles in the small angle region of compound **4** in the SmA and SmA′ phases. The layer

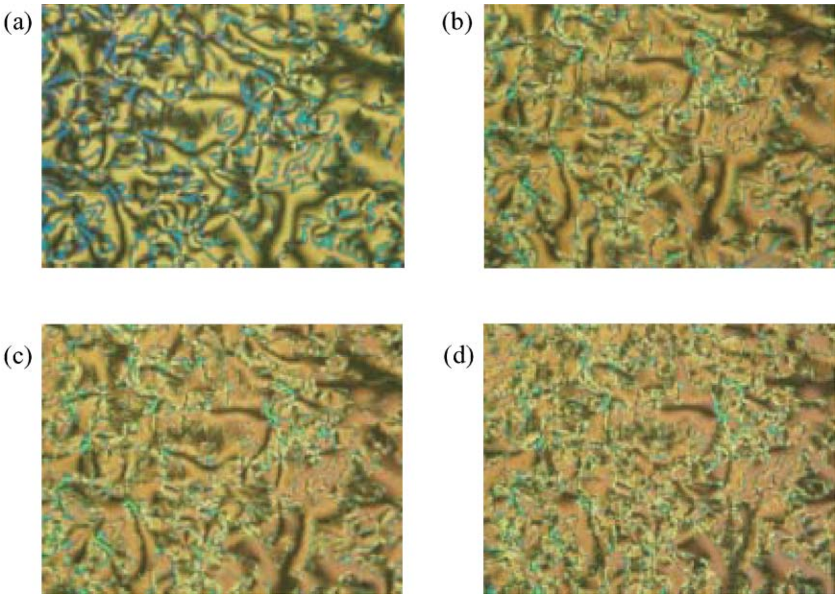

Fig. 7 Photomicrographs of (a) the N phase at 105 °C, (b) the SmX phase at 90 °C, (c) the SmY phase at 75 °C and (d) the SmZ phase at 60 °C of a uniform planarly aligned sample of compound **5**. Magnification 100 ×.

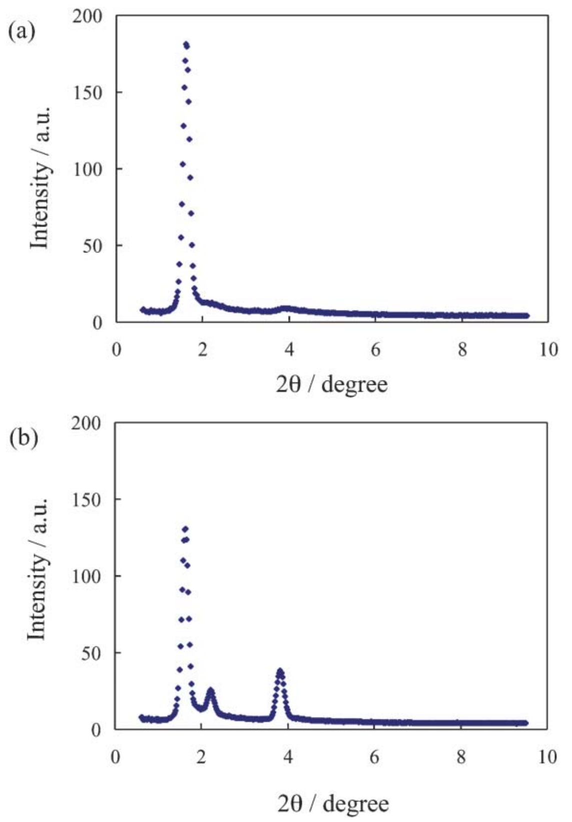

Fig. 9 X-Ray diffraction patterns of compound **4** in (a) the SmA phase at 162 °C and (b) the SmA′ phase at 148 °C.

spacing of the SmA phase of compound **4** was 53 Å, but the molecular length was estimated to be 40 Å, suggesting the formation of an interdigitated phase.[11] The SmA′ phase showed a complicated X-ray pattern. In the SmA′ phase at 148 °C three sharp reflections, 2θ = 1.62°, 2.20° and 3.82°, were observed in the small angle region, corresponding to the spacings of about 55 Å, 40 Å and 23 Å, respectively (Fig. 9). The 2D pattern of the aligned sample in the SmA′ phase showed that three reflection peaks in the small angle region are positioned at one direction perpendicular to the diffuse scattering in the wide angle region (Fig. 10). These results strongly indicate that the SmA′ phase is an incommensurate SmA (SmAinc) phase in which three periodic density waves co-exist along the layer normal.[12–14] In the X-ray pattern of the SmA phase (Fig. 9(a)), two small peaks are recognized to locate at the same positions as observed in the SmA′ phase (Fig. 9(b)). These results suggest that weak density waves with the same periodicity as the SmA′ phase may co-exist in the SmA phase.

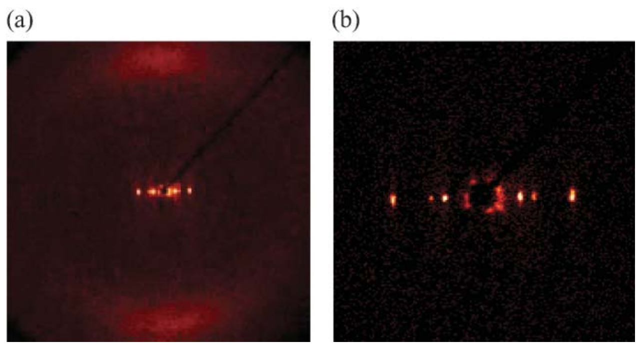

Fig. 10 (a) X-Ray diffraction patterns of an aligned sample of compound **4** at 148 °C and (b) its expanded one.

In order to investigate the stability of the SmAinc phase, some miscibility studies were performed. Fig. 11 shows transition temperatures of binary mixtures of compound **4** (50 mol%) with each of some cyanobiphenyl derivatives. Both **1OCB** and **6OCB** showed the N phase, whereas **2-CN** did not exhibit liquid-crystalline phases. Addition of 4,4′-dicyanobiphenyl (**2-CN**) or 4-cyano-4′-methoxybiphenyl (**1OCB**) to compound **4** was found to stabilize the SmAinc phase. However, addition of 4-cyano-4′-hexyloxybiphenyl (**6OCB**) removed the SmAinc phase. These results indicate that the SmAinc phase organized by compound **4** can recognize the difference in molecular length between **1OCB** and **6OCB**. Furthermore, the SmAinc was stabilized even in the mixture containing 66 mol% of **2-CN**. Transition temperatures for the mixture were Iso Liq 180 °C N 165 °C SmAinc 81 °C recryst. Three sharp reflections in the small angle region of the mixture at 157 °C were detected and the obtained layer spacings were 52, 39, and 23 Å. The three periodic density waves in the SmAinc phase of compound **4** were not destroyed in the mixture containing 66 mol% of **2-CN**. This system shows a new type of inclusion phenomenon.

Let us discuss a possible model for the SmAinc phase. Fig. 12 shows a grand state conformer obtained from MM2 calculations, which shows a λ-shaped structure. Although the molecule should keep the molecular flexibility and stability of the conformer from MM2 calculations is still questionable, we consider the single conformer to discuss the phase structure at the first approximation. A periodicity of 40 Å which is corresponding to the molecular length results from a monolayer structure (Fig. 13 (a)). That of 23 Å is attributed to a layer spacing of an intercalated structure (Fig. 13(b)). The intercalated structure seems to be unrealistic, because it contains many voids. A layer spacing of 55 Å in the SmAinc phase, longer than the molecular length, suggests the existence

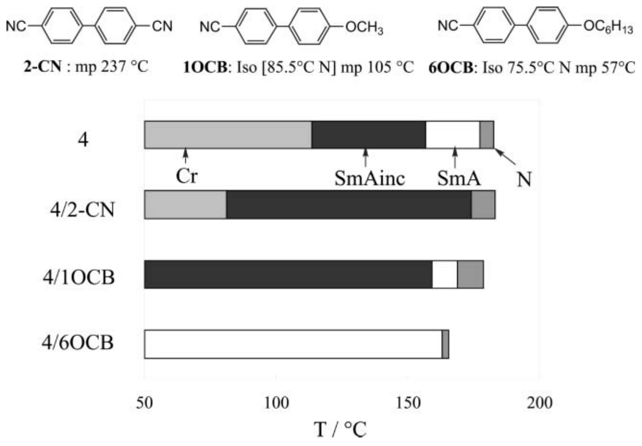

Fig. 11 Transition temperatures of binary mixtures of compound **4** (50 mol%) with each of some cyanobiphenyl derivatives. Temperatures were determined by polarized light microscopy on cooling.

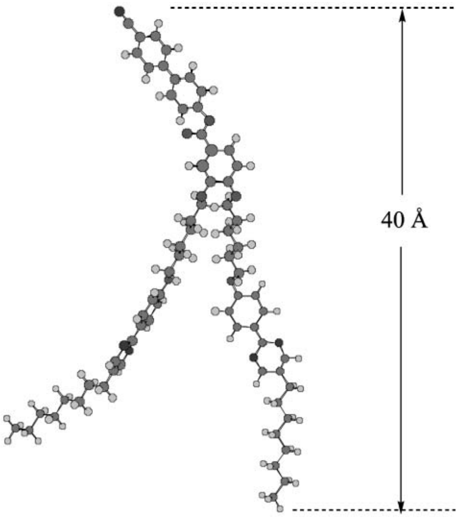

Fig. 12 Conformation of compound **4** obtained from MM2 calculations.

of an interdigitated structure. Two different interdigitated structures can be considered (Fig. 14). Interactions between cyanobiphenyl and phenylpyrimidine moieties can be seen in Fig. 14(a). On the other hand, there are dipole–dipole interactions between cyanobiphenyl moieties and those between phenylpyrimidine moieties in Fig. 14(b). Although there are unfavorable free volumes in the interdigitated structure (Fig. 14(b)), the structure seems to be realistic. This is because the electron density is less localized in Fig. 14 (b) compared with Fig. 14(a) and this is consistent with the absence of second order layer diffraction in the X-ray pattern of compound **1** in the SmAinc phase. Furthermore, if the other monolayered and intercalated structures are superimposed onto the interdigitated structure, the unfavorable free volumes can be reduced to some extent and the interdigitated structure (Fig. 14(b)) be stabilized. Thus, the coexistence of three different molecular packings, corresponding to the monolayer, intercalated and interdigitated structures, can be proposed as a possible model of the observed SmAinc phase.

Compound 5

The X-ray pattern of compound **5** in the SmX phase shows two relatively broad reflections, $2\theta = 2.60°$ and 3.35°, in the small angle region, corresponding to spacings of about 34 Å and 26 Å, respectively. However, a diffuse scattering in the wide-angle region was observed, which indicates the fluid state of the mesophase (Fig. 15). The origin of the two reflections in the SmX phase is not clear; however, at least two density waves coexist. The molecular length was estimated to be 53 Å. The shorter layer spacings than the molecular length indicate that an intercalated structure occurs in the SmX phase.[11] Two density waves were also observed in the SmY and SmZ phases but a layer structure with longer periodicity is stronger than the other.

Let us discuss the structure of the SmX phase. By means of the optical microscopic studies, the SmX phase is an optically uniaxial phase but the Schlieren-like texture was observed in the uniform planarly aligned sample. A Schlieren texture is usually observed in a uniform planarly aligned sample of a N phase, which results from deformation of the n-director, and in a homeotropically aligned sample of a tilted smectic phase, which results from that of the c-director. The Schlieren-like texture observed in the uniform planarly aligned sample of the SmX phase can result from bend deformation of the n-director, which is thought to be forbidden in smectic phases. The two relatively broad reflections in the small angle region in the SmX phase of compound **5** indicate that: (i) two different density waves coexist and (ii) both of the layer periodicities are weak. The shorter layer spacing than the molecular length

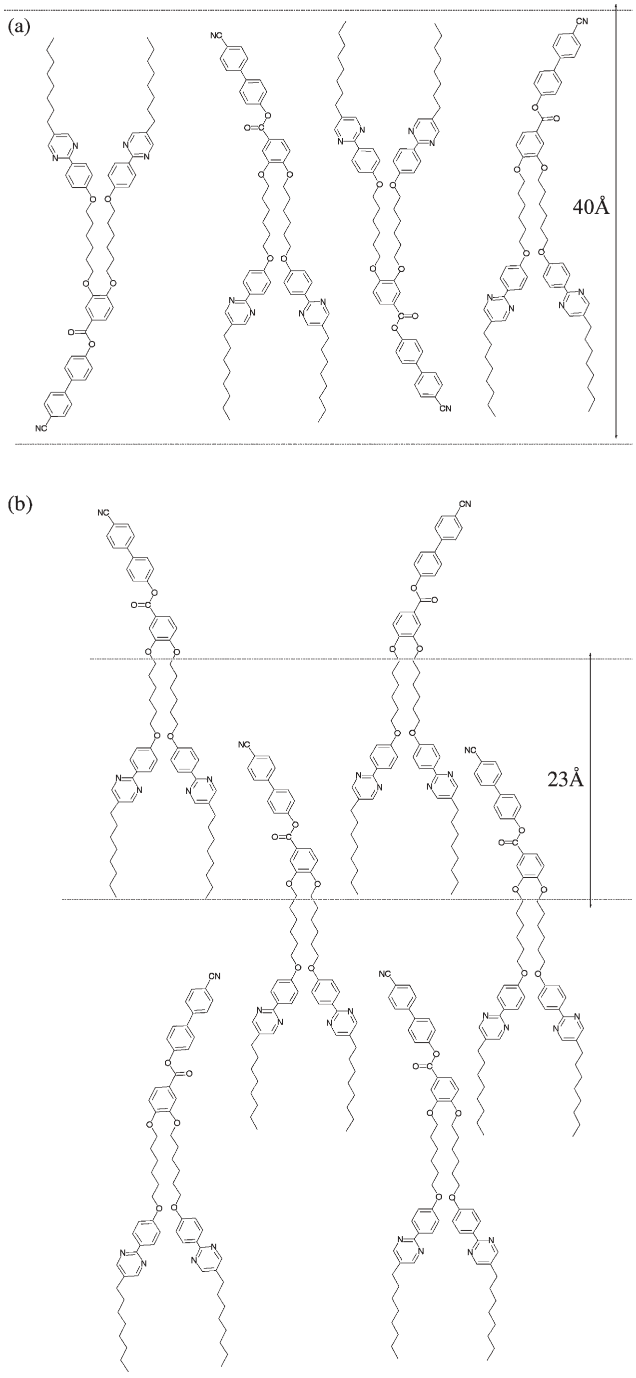

Fig. 13 Possible models of monolayer and intercalated structures for the SmAinc of compound **4**.

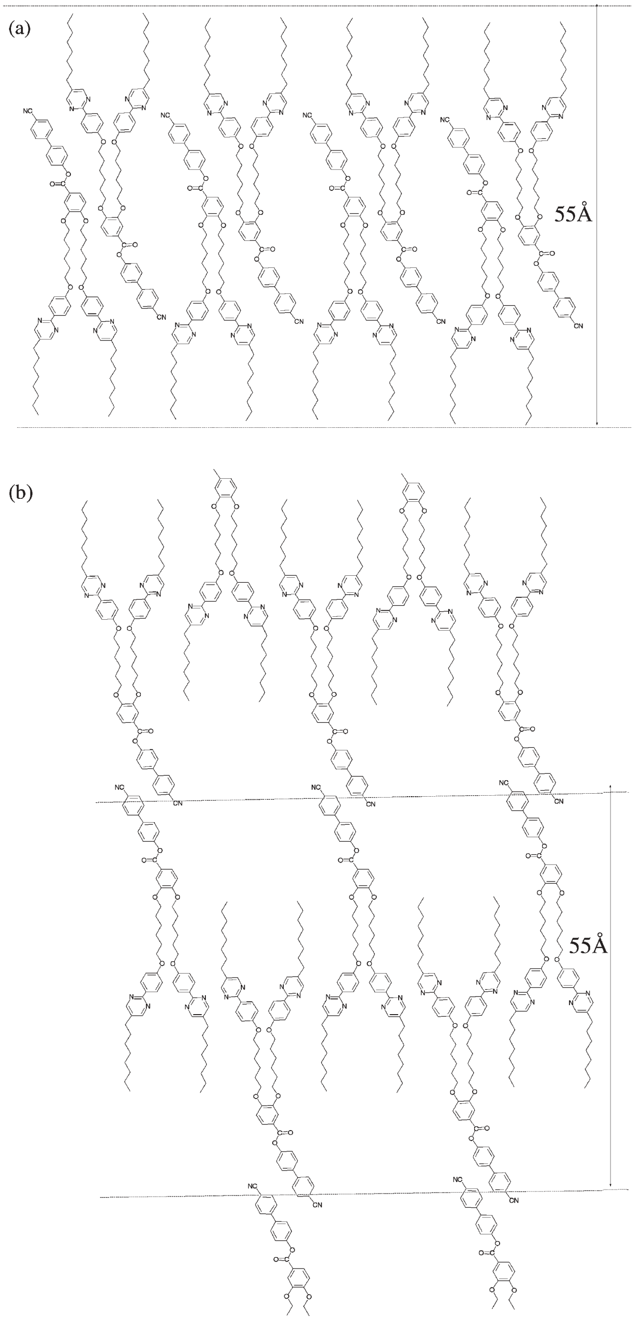

Fig. 14 Possible models of two different interdigitated structures for the SmAinc phase of compound **4**.

suggests an intercalated structure. The molecules in the SmX phase are considered to have relatively higher mobility along the layer normal than those in a conventional SmA phase. Thus, the Schlieren texture produced by the deformation of the n-director in the N phase can remain even in the layered molecular assembly produced in the SmX phase.

In order to investigate the interactions between phenylpyrimidine groups, compounds **6**, **7** and **8** were prepared and the transition properties compared with those of compound **5** (Fig. 16). Compounds **6**, **7** and **8** did not show the unusual phases observed for compound **5**. Compound **6** showed only a SmA phase in which a typical fan texture was observed.

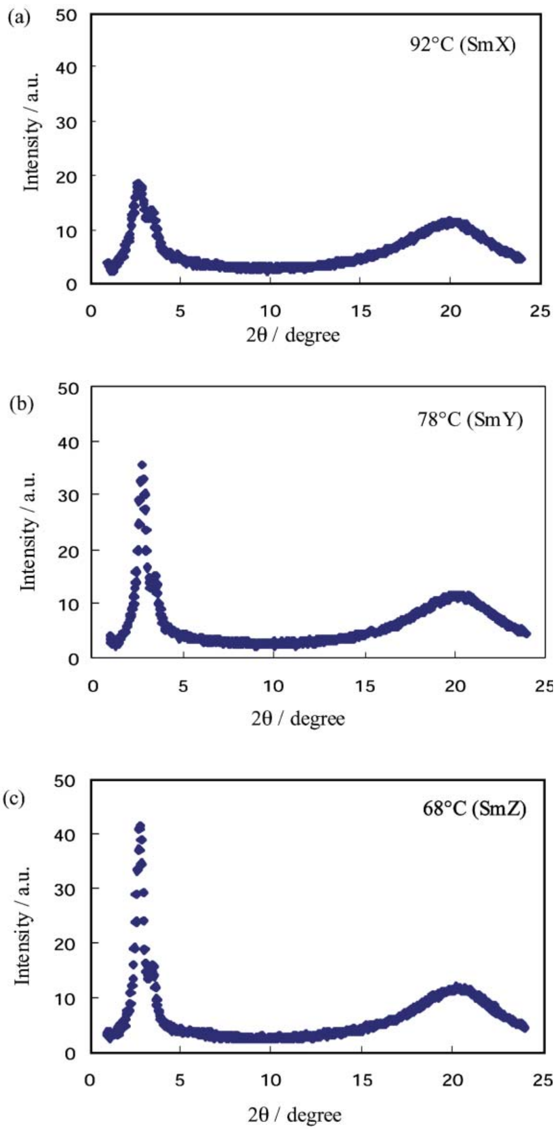

Fig. 15 X-Ray diffraction patterns for compound **5** in (a) the SmX phase at 92 °C, (b) the SmY phase at 78 °C and (c) the SmZ phase at 68 °C.

Compound **7** showed a phase sequence of Iso–SmA–SmC–Cr, but compound **8** showed that of Iso–SmC–Cr. These results indicate that the anti-parallel orientation of the phenylpyrimidine groups between adjacent molecules plays an important role in the anomalous molecular organization observed in compound **5**. Furthermore, if the overall molecular configuration of compound **5** were Y-shaped, the transition behaviour of compound **7** should be similar to that of compound **8**, because a Y-shaped molecule should have a C_2 axis along the molecular long axis. The marked difference in the transition behaviour between compounds **7** and **8** suggests that the molecular shape is not Y-shaped but λ-shaped. A possible molecular arrangement responsible for the appearance of the Schlieren-like in the SmX phase is shown in Fig. 17. This unique molecular assembly is considered to be stabilized by several types of anti-parallel interactions between the phenylpyrimidine groups. Effective packing of the λ-shaped

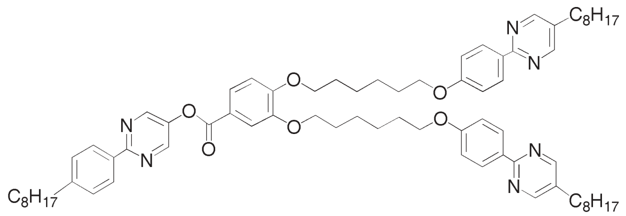

6 : Iso 158 (5.7) SmA mp 128

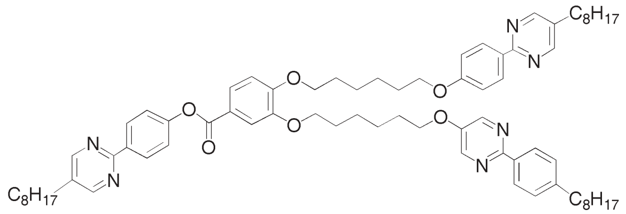

7 : Iso 171 (8.9) SmA 166 SmC mp 137

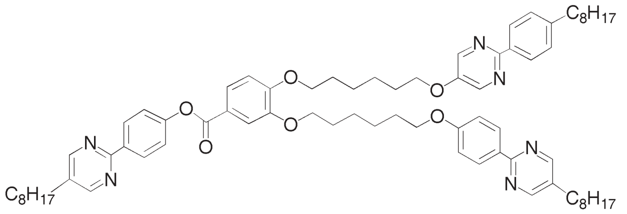

8 : Iso 162 (6.8) SmC mp 115

Fig. 16 Molecular structure, phase transition temperatures/°C and $\Delta S/R$ (in parenthesis) of compounds **6**, **7** and **8**.

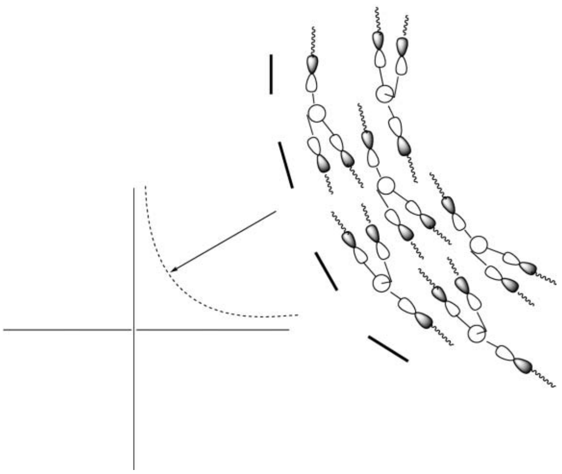

Fig. 17 A possible model for the molecular orderings producing a Schlieren texture of the SmX phase of compound **5**.

molecules and the electrostatic forces, both polar and quadrupolar, between the phenylpyrimidine groups make it possible to produce bend deformation of the layer structure.

Characteristic molecular assembly organized by λ-shaped mesogenic molecules

Many types of liquid crystals with unconventional molecular shapes have been reported.[15] For example, Göring *et al.* reported tuning-fork shaped molecules which show undulated smectic structures[16] and Attard *et al.* reported Y-shaped molecules in which three mesogenic groups are symmetrically attached to a phenyl ring.[17] As discussed above, the transition behaviour and the phase structures shown by the present λ-shaped molecules are different from those of the liquid-crystalline materials so far reported. Thus, in the final part of this article, we consider intermolecular interactions of the λ-shaped structures and highlight the unique features produced by the λ-shaped molecules.

Phase transition behaviour depends on the structure of X. Compounds **1** and **3** showed a monolayer SmA phase. The most important factor for the organization in the SmA phase of both compounds is steric interactions due to the particular shape of the molecules. In the case of compound **4**, dipole–dipole interactions through cyanobiphenyl groups and anti-parallel interactions through phenylpyrimidine groups is responsible for producing the incommensurate SmA phase with interdigitated structure. On the other hand, on introduction of a phenylpyrimidine group as X (compound **5**), several types of anti-parallel interactions between phenylpyrimidine groups can produce the unusual phases with intercalated structure in which the layer ordering and the deformation of the n-director coexist. This nature surely increases the penetration length[18] of the n-director perturbation when the bending deformation is imposed in a system. Thus, the λ-shaped configuration is one possible molecular design realizing a dislocation-driven "bend grain boundary" phase[19] which was predicted[18] but has not yet been observed. The proper arrangement of the mesogenic parts in a particular λ-shaped structure regulates the inter-layer and intra-layer interactions, and thus can produce a variety of novel molecular aggregation styles.

Conclusions

The newly designed λ-shaped mesogenic molecules were found to realize a novel class of exciting molecular organization in liquid crystalline phases, *i.e.*, a stable incommensurate SmA phase and a liquid-crystalline phase in which the layer ordering and the deformation of the n-director coexist. The SmAinc phase can include a large amount of 4, 4′-dicyanobiphenyl which does not show a liquid-crystalline phase. Furthermore, the SmAinc phase was found to recognize difference in molecular length between **1OCB** and **6OCB**. Modification of the λ-shaped structure can produce various organizations of molecules.

Acknowledgements

We thank Dr Lianhui Qi of Yokoyama Nano-structured Liquid Crystal Project for XRD measurements. This work was partly supported by a Grant-in Aid for Scientific Research from the Ministry of Education, Science, Sports, Culture, and Technology in Japan (No. 15550156).

Akihisa Yamaguchi,[a] **Isa Nishiyama,**[b] **Jun Yamamoto,**[b]
Hiroshi Yokoyama[b] **and Atsushi Yoshizawa***[a]
[a]*Department of Materials Science and Technology, Faculty of Science and Technology, Hirosaki University, 3 Bunkyo-cho, Hirosaki 036-8561,*

Japan. E-mail: ayoshiza@cc.hirosaki-u.ac.jp
[b] *Yokoyama Nano-structured Liquid Crystal Project, ERATO, JST, TRC 5-9-9 Tokodai, Tsukuba 300-2635, Japan*

References

1 J. W. Goodby, G. H. Mehl, I. M. Saez, R. P. Tuffin, G. Mackenzie, R. Auzely-Velty, T. Benvegu and D. Plusquellec, *Chem. Commun.*, 1998, 2057.
2 (*a*) C. Tschierske, *J. Mater. Chem.*, 1998, **8**, 1485; (*b*) C. Tschierske, *J. Mater. Chem.*, 2001, **11**, 2647.
3 I. M. Saez and J. W. Goodby, *Chem. Commun.*, 2003, 1726.
4 M. Prehm, X. H. Cheng, S. Diele, M. K. Das and C. Tschierske, *J. Am. Chem. Soc.*, 2002, **124**, 12072.
5 A. Yoshizawa, H. Kikuzaki and M. Fukumasa, *Liq. Cryst.*, 1995, **18**, 351.
6 A. Yoshizawa, J. Umezawa, N. Ise, R. Sato, Y. Soeda, T. Kusumoto, K. Sato, T. Hiyama, Y. Takanishi and H. Takezoe, *Jpn. J. Appl. Phys.*, 1998, **37**, L942.
7 A. Yoshizawa and A. Yamaguchi, *Chem. Commun.*, 2002, 2060.
8 A. Yoshizawa, K. Yamamoto, H. Dewa, I. Nishiyama, J. Yamamoto and H. Yokoyama, *J. Mater. Chem.*, 2003, **13**, 172.
9 V. Faye, H. T. Nguyen, V. Laux and N. Isart, *Ferroelectrics*, 1996, **179**, 9.
10 I. Nishiyama, T. Yamamoto, J. Yamamoto, J. W. Goodby and H. Yokoyama, *J. Mater. Chem.*, 2003, **13**, 1868.
11 C. T. Imrie and G. R. Luckhurst, in the *Handbook of Liquid Crystals*, ed. D. Demus, J. W. Goodby, G. W. Gray, H. -W. Spiess and V. Vill, Wiley-VCH, Weinheim, 1998, vol 2B, ch. X, pp. 801–833.
12 J. M. Seddon, in the *Handbook of Liquid Crystals*, ed. D. Demus, J. W. Goodby, G. W. Gray, H. -W. Spiess and V. Vill, Wiley-VCH, Weinheim, 1998, vol. 1, ch. VIII, pp. 635–679.
13 J. T. Mang, B. Cull, Y. S. Shi, P. Patel and S. Kumar, *Phys. Rev. Lett.*, 1995, **74**, 4241.
14 (*a*) F. Hardouin, M. F. Achard, J. L. Jin, J. W. Shin and Y. K. Yun, *J. Phys. II*, 1994, **4**, 627; (*b*) F. Hardouin, M. F. Achard, J. L. Jin and Y. K. Yun, *J. Phys. II*, 1995, **5**, 927.
15 D. Demus, in *Handbook of Liquid Crystals*, ed. D. Demus, J. W. Goodby, G. W. Gray, H. -W. Spiess and V. Vill, Wiley-VCH, Weinheim, 1998, vol. 1, ch. VI, pp. 133–187.
16 P. Göring, G. Pelzl, S. Diele, P. Delavier, K. Siemensmeyer and K. H. Etzbach, *Liq. Cryst.*, 1995, **19**, 629.
17 G. S. Attard, A. G. Douglass, C. T. Imrie and L. Taylor, *Liq. Cryst.*, 1992, **11**, 779.
18 P. G. de Gennes, *Solid State Commun.*, 1972, **10**, 753.
19 H.-S. Kitzerow, in *Chirality in Liquid Crystals*, ed. H.-S. Kitzerow and C. Bahr, Springer-Verlag, New York, 2001, pp. 346–347.